On Collaborative Robot Teams for Environmental Monitoring: A Macroscopic Ensemble Approach

Victoria Edwards, Thales C. Silva, Bharg Mehta, Jasleen Dhanoa, and M. Ani Hsieh

***Abstract*— With the rapidly changing climate and an increase in extreme weather events, it is necessary to have better methods to monitor and study the impacts of these phenomena on urban river environments. Multi-robot environmental monitoring has long focused on strategies that assign individual robots to distinct regions or task objectives. While these methods have seen success for Autonomous Surface Vehicles (ASVs), the spatial expanse and temporal variability of rivers impose an increased burden on existing techniques, necessitating computationally intensive replanning. Alternative methods aim to model and control teams of robots by prescribing global constraints on the system, using the insight that robots' transitions between tasks are stochastic and time-based. These methods do not require replanning because robots will perform different tasks achieving the overall desired system state, focusing on temporal switching alone limits their overall descriptive power. In this paper, we present a method that considers collaborations between robots to inform task switching based on spatial proximity. Our results suggest that in unknown environments macroscopic models provide increased flexibility for individual robot task execution as compared to coverage control methods.**

***Index Terms*— Macroscopic models, Robotic Teams, Environmental Monitoring**

I. Introduction

Urban centers are often established in proximity to rivers which provide people access to diverse resources [1], [2]. The health of the ecosystems in these environments necessitates better understanding of the impact of human activities in and around these areas, *e.g.*, how pollutants resulting from agriculture and/or waste water runoffs hinder natural river regulation processes [3], [4]. Additionally, other climate change driven events including rising sea levels and increased rainfall [5], can impact the shape of the river interfering with urban river infrastructure such as bridges [6]. In this work, we consider environmental monitoring strategies of unknown environments that require flexible replanning to match environmental changes.

Given the dynamic nature and large spatial expanse of most rivers, multi-robot systems, particularly ones including autonomous surface vehicles (ASVs), are often employed in their monitoring [7]–[11]. These methods focus on planning and control for the individual robot, or are bottom-up approaches to working with multi-robot teams. Existing bottom-up multi-robot environmental monitoring strategies focus on two main approaches. The first method, aims to assign robots to tasks which requires solving an NP-Hard combinatorial optimization problem [12], [13]. Alternatively, coverage based approaches often rely on a tessellation of the environment in which robots are assigned regions to monitor [7], [14]. The limitation of bottom-up methods is the lack of formal analysis describing the overall behavior of the system, resulting in *ad hoc* evaluation of the robot team. In addition, these methods often require computationally expensive replanning to handle new information about the environment. This replanning either requires global knowledge of the state of the system or communication methods for robots to determine how to redistribute resources [14], [15].

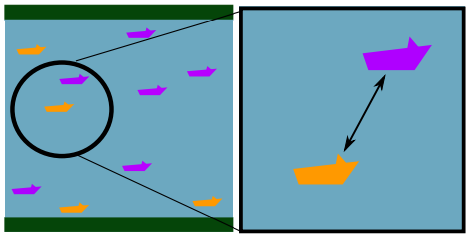

Fig. 1: During environmental monitoring on a river, robots will interact spatially. This interaction can result in collaboration, *i.e.*, task switching, depending on how many other robots are performing the task and the overall goal of the system.

Another way to design single robot task execution strategies for environmental monitoring by a team of robots is to employ a top-down macroscopic ensemble approach. Such an approach enables the specification of global behaviors for the team *a priori* while enabling individual robots to switch between tasks without the need for replanning. The ability to model the global dynamics of the robot team has led to insights into the stability, scalability, and the design of feedback control strategies for these systems [16], [17], but often at the cost of ignoring the specific complexities of individual robot dynamics and their interactions with other robots and the environment. This is because the derivation of the macroscopic ensemble models relies on the assumption that individual robot models can be abstractly represented as stochastic hybrid systems and as such robots effectively switch between their assigned tasks in a time-based stochastic fashion [18]. Nevertheless, these models have proven to be extremely powerful in improving the performance of large teams of robots tasked to execute a collection of spatially distributed single-robot tasks [19]–[21].

While macroscopic approaches have been employed for collaborative tasks, *i.e.*, tasks where robots must work in

We gratefully acknowledge the support of NSF IUCRC 1939132, the University of Pennsylvania's University Research Foundation Award, and the National Defense Science & Engineering Graduate (NDSEG) Fellowship.

Victoria Edwards, Thales C. Silva, Bharg Mehta, Jasleen Dhanoa and M. Ani Hsieh are with Department of Mechanical Engineering and Applied Mechanics and the GRASP Laboratory, University of Pennsylvania, PA, 19104, USA {vmedw,scthales,bharg,jkdhanoa,mya}@seas.upenn.edu

conjunction with other robots [22], these methods are fundamentally limited by only considering the time a task must be done together with another robot instead of collaborations as the result of spatially based interactions. Similar to [23], we consider an environmental monitoring task where task switching occurs based on potential collaborations with other team members. However, our proposed approach uses an abstracted model to describe robot collaboration-informed task switching between different behavioral patterns. Figure 1 shows an example spatial interaction and the result of this interaction is a potential collaboration based on the desired global state of the system. The contributions of this paper are: (i) A nonlinear macroscopic ensemble model for environmental monitoring based on robot collaboration to inform behavior switching. (ii) Analysis of the proposed model and control strategies to improve the robustness of the robotic team. (iii) Comparison of the macroscopic ensemble environmental modeling with other existing solutions, and evaluation on data collected during ASV surveys on the Schuylkill River in Philadelphia PA, [24].

II. Problem Formulation

Given a team of autonomous surface vehicles we aim to define a macroscopic ensemble model and control approach to execute environmental monitoring in a river environment.

A. Single Robot Exploration-Exploitation Behaviors

Consider individual robots which are capable of executing different path planning strategies to achieve behaviors necessary for environmental monitoring. We will refer to behaviors and tasks interchangeably to mean the specific pattern the robot is executing. Let $M = 3$ tasks be performed by a team of N robots. The three tasks are home, explore, and exploit, where any robot performing a task has a specific path pattern to execute. These task categories are well known and provide a starting point for the more general study of collaborative macroscopic ensemble models that may consist of more complex behavioral patterns.

A directed graph $\mathcal{G} = (\mathcal{V}, \mathcal{E})$ is built to represent the relation between tasks, Figure 2a. This graph $\mathcal{G}$, is connected in a cycle between the three tasks, where from home robots go to the explore task, from explore robots go to the exploit task, and from the exploit task robots go home. The elements of the node set $\mathcal{V} = \{v_1, v_2, v_3\}$ corresponds to each task, and the elements of the edge set $\mathcal{E} \subset \mathcal{V} \times \mathcal{V}$ corresponds to possible changes between tasks. Specifically, an edge $e_{ij} \in \mathcal{E}$ can be either zero, if robots cannot switch from task v_i to task v_j, or $e_{ij} = 1$ if the switch from task v_i to task v_j is allowed. We assume that graph $\mathcal{G}$ is strongly connected, which means that there is a path from each task to any other task in the graph. Prior work has used task graphs to represent spatially distributed tasks [17], [20], however, in our instance, $\mathcal{G}$ is reflective of the potential for robot collaboration to occur. For collaboration to exist between robots performing different tasks, the robots performing tasks must be *well-mixed*. We define *well-mixed* as the *sufficiently* even dispersal of robots performing tasks in a bounded workspace, such that robots are likely to come within collaboration range [25].

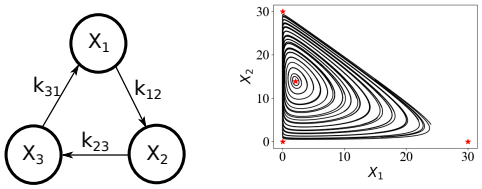

(a) Task Graph (b) Phase Portrait

Fig. 2: Figure 2a is a task graph for an exploration-exploitation scenario. Figure 2b shows numerical simulations for various initial populations with the constraint that $N = 30$, and $k_{12} = k_{31} = 0.002$ and $k_{23} = 0.0003$.

B. Macroscopic Ensemble Model

Consider our outlined environmental monitoring scenario with $M = 3$ tasks and N robots. We define a transition law that determines the outcome of a collaboration between two robots performing different tasks. The population of each behavior is represented by a random variable X_i, and the dynamics can be written as:

$$\begin{aligned} \dot{X}_1 &= -k_{12}X_1X_2 + k_{31}X_1X_3, \\ \dot{X}_2 &= -k_{23}X_2X_3 + k_{12}X_2X_1, \\ \dot{X}_3 &= -k_{31}X_3X_1 + k_{23}X_3X_2, \end{aligned} \tag{1}$$

where each population $X_i > 0$ for all time and k_{12}, k_{31}, k_{23} are collaboration rates between robots performing the three tasks. Note that for each edge, e_{ij}, $\dot{X}_i$ has a positive term representing the addition of robots to task i, $k_{ij}X_iX_j$, and the same term appears in $\dot{X}_j$ as a negative term representing the loss of robots from task j.

We assume a fixed population of N robots which means we need to guarantee that $\sum_i^3 X_i = N$ for all time. We will use similar model analysis techniques to those used in in evolutionary biology to guarantee our constraint [26], [27]. Consider the two dimensional simplex as,

$$\triangle_2 = \{X \in \mathbb{R}^3 | X_i \geq 0,\ X^T\mathbf{1} = N\}, \tag{2}$$

where $\mathbf{1}$ is a vector of ones of dimension $\mathbb{R}^3$. Let $X = \begin{bmatrix} X_1 & X_2 & X_3 \end{bmatrix}^T$, and $f(X) = \begin{bmatrix} f(X_1) & f(X_2) & f(X_3) \end{bmatrix}^T$, where $f_i(X) = \dot{X}_i$. We know $X^T\mathbf{1} = N$ from the definition of the system, likewise $\mathbf{1}^T f(X) = 0$, which implies that $X^T\mathbf{1} = N$ is an invariant hyperplane, since $X^T\mathbf{1}$ is non-negative. Therefore, the positive quadrant of $\mathbb{R}^3$ is a trapping region for the dynamics, *i.e.,* all trajectories starting with positive populations of robots, $X_i > 0$ for all $i \in \mathcal{V}$, will remain positive. In addition, the intersection of the invariant hyperplane and the positive quadrant of $\mathbb{R}^3$ reduces the system to the 2 dimensional simplex, $\triangle_2$. This reduction allows for the following model simplification, where $X_3 = (N - (X_1 + X_2))$ and the new system of equations is as follows:

$$\begin{aligned} \dot{X}_1 &= -k_{12}X_1X_2 + k_{31}X_1(N - (X_1 + X_2)), \\ \dot{X}_2 &= -k_{23}X_2(N - (X_1 + X_2)) + k_{12}X_2X_1. \end{aligned} \tag{3}$$

We have described a macroscopic ensemble method to model the distributions of robots performing the three different

environmental monitoring tasks, at the microscopic level robots will switch between tasks based on local collaborations. We will now study the behavior of Equations (3), and introduce control methods to ensure that our desired outcomes are achieved.

III. Analysis and Control

The equilibrium points for Equations (3) are: $\big[0, N\big]$, $\big[N, 0\big]$, $\big[0, 0\big]$, and $\left[\frac{k_{23}N}{k_{12}+k_{23}+k_{31}}, \frac{k_{31}N}{k_{12}+k_{23}+k_{31}}\right]$. Notice that there are three equilibrium at the extreme points of the simplex $\triangle_2$, red stars in Figure 2b. We determine the local stability of each fixed point (see Chapter 6 of [28] for more details). Consider $k_{ij} > 0$ for all $i, j \in \{v_1, v_2, v_3\}$, in this case the first three fixed points are unstable. Specifically, the eigenvalues of the Jacobian matrix evaluated on those points have one positive and one negative real values (*i.e,* saddle points [28]). The final equilibrium has a pair of complex conjugate eigenvalues suggesting center classification, or closed loop orbits that neither attract nor repel trajectories around the equilibrium, *i.e.* neutrally stable [28]. For the purposes of this work, we select parameters which result in close to center behavior, as seen in Figure 2b. However, further detailed analysis is needed to classify the equilibrium for all model parameters. For $k_{ij} < 0$ for all i, j, the direction of the graph is reversed and the fixed point classification is the same as before. Finally, if $k_{ij} = 0$ for any pair i, j in (1), the strongly-connected assumption on $\mathcal{G}$ is invalidated.

The proposed model with our chosen parameters is sensitive to population size fluctuations, which are likely to arise during microscopic evaluation. Such sensitivity means that it is easy to lose small populations of robots performing certain task behaviors.

Claim 1: If any X_i gets too small, the result is a shift in the behavior of the equilibrium points for Equations (1). Consider if any $X_i = 0$ in Equation (1), to find the new equilibrium point at least one other population must be 0, $X_j = 0$. Because we are in a trapping region, as specified before this implies that all robots must be attracted to the remaining behavior such that $X_k = N$. Thus we have the loss of two behaviors. Notice that as any population gets small, the system tends towards the extreme points of the simplex, which implies that at least one task is no longer being performed. This motivates the need to consider control strategies which can help recover the lost task behavior.

A. Control Synthesis

To help mitigate and/or reverse task loss we present two control strategies. Our first method, is to allow robots performing the same task to switch to a new task when they are within collaboration range, specifically $X_i + X_i \xrightarrow{k_{ii}} 2X_j$, where $j = \mod(i+1, M)$, *i.e.,* the next task in the graph.

$$\begin{aligned}\dot{X}_1 =& -k_{12}X_1X_2 + k_{31}X_1(N-(X_1+X_2)) \\ & - k_{11}X_1^2 + k_{33}(N-(X_1+X_2))^2 \\ \dot{X}_2 =& -k_{23}X_2(N-(X_1+X_2)) + k_{12}X_2X_1 \\ & - k_{22}X_2^2 + k_{11}X_1^2, \end{aligned} \tag{4}$$

where k_{ii} is the self collaboration rate for robots performing the same task. The addition of the self collaborating terms changes the system dynamics to a stable attractor, and is referred to as Control 1 (C1) in Section V. For example, if many robots are performing the exploitation task in the same region then this type of collaboration will help robots move back to the home behavior.

Our second method is to use the well-studied time based task switching, [17], [18], which at the microscopic level can be translated to robots changing tasks after a certain amount of time, specifically $X_i \xrightarrow{p_{ij}} X_j$ where p_{ij}, is a transition rate from robots performing task i to task j. The resulting dynamical system is

$$\begin{aligned}\dot{X}_1 =& -k_{12}X_1X_2 + k_{31}X_1(N-(X_1+X_2)) + p_{21}X_2 \\ & + p_{31}(N-(X_1+X_2)) - (p_{12}+p_{13})X_1 \\ \dot{X}_2 =& -k_{23}X_2(N-(X_1+X_2)) + k_{12}X_2X_1 + p_{12}X_1 \\ & + p_{32}(N-(X_1+X_2)) - (p_{21}+p_{23})X_2. \end{aligned} \tag{5}$$

Previous work by Berman *et al.* [18] and Silva *et al.* [17] showed that the dynamics of the linear macroscopic ensemble models result in stable distributions of X_i for a given set of parameters p_{ij}. The result for Equations (5) is that the linear terms dominate the dynamics and drive the system to a stable equilibrium. This control method is referred to as Control 2 (C2) in Section V.

Thus both control methods result in final distributions of robots which settle to around an equilibrium, this means that for all time robots will continue to perform all three of the specified tasks. In addition, the recovery of behaviors is possible because the control terms can reintroduce lost behaviors back into the system organically.

IV. Experimental Setup

A. Experimental Data Collection

In the summer of 2022, field deployments using the Clearpath Heron ASV in the Philadelphia, PA, Schuylkill River were performed [24], Figure 3a. The data collected consists of ASV trajectories using the onboard DGPS and vectorNav IMU for localization, and a Micron Echosounder to measure depth data of the river. Rivers are impacted by tidal fluctuations which will change the observed river depth by the bathymetry sensor. As such, we perform tidal corrections using linear interpolation between high and low tides with data from tide tables for the Schuylkill River [29]. The tide correction was computed to consider all data at low tide, the resulting cleaned up dataset is in Figure 3b.

To evaluate multi-robot river exploration-exploitation strategies we need to interpolate between the sampled data points in the dataset. To the best of our knowledge, there is no prior work studying the Schuylkill River, so we used Scikit Learn Gaussian Process Regression (GP) [30], a non-parametric modeling approach to approximate the underlying function that describes the data. We invite others to use our dataset: `https://github.com/hsiehScalAR/Schuylkill_River_Dataset`.

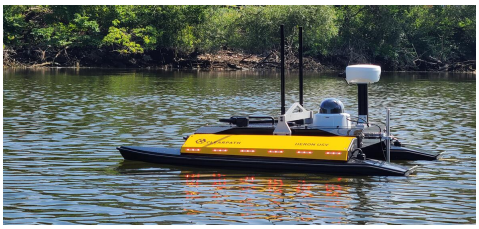

(a) A Clearpath Heron on the Schuylkill River in Philadelphia, PA. This photo was taken by T. Z. Jiahao.

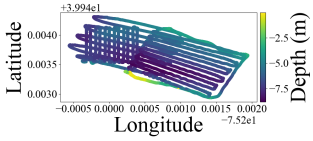

(b) Raw data

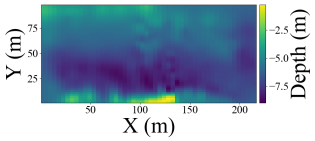

(c) Interpolated data

Fig. 3: Figure 3b is the raw data from 4 experimental surveys, and Figure 3c is the combined interpolated map solved with Scikit Learn Gaussian Process Regression [30]. Color corresponds to depth in both cases.

B. Evaluation Methods

Our simulated platforms are point robots that follow assigned waypoints. Using the environmental monitoring scenario we have outlined, we can define specific instantiations of each task behavior pattern while being careful to ensure our well-mixed assumptions. Robots performing the home task do not collect data and go to any next location assigned within the workspace. Robots executing the exploration task will perform a random walk within the workspace, and robots at the exploitation task switch a third of the way through the experiment from circling at random locations to a greedy exploit where the robot goes to the deepest point observed so far and circles. In environmental monitoring the aim is to collect high-value information, we use depth as the richest form of information in our current dataset and it could be replaced by other high value sensor measurements, [31].

To apply this method to robots it is necessary to map the macroscopic model parameters to the individual robot. Collaboration rates, k_{ij}, are related to the density of robots in a fixed environment, the collaboration area for robots performing different tasks is given by,

$$A_{ij} = \frac{k_{ij} N \Omega A \sqrt{A}}{v_{ij} X_i X_j}, \tag{6}$$

where A is the total area robots will collaborate, k_{ij} is the collaboration rate, v_{ij} is the average relative speed between robots performing different tasks, and Ω is an approximate scaling coefficient of the robot area to the environment size. Notice that robots *will* switch tasks whenever they come within the collaboration area of each other, and also (6) takes into account the population of robots performing adjacent tasks. As the size of the environment increases the only way to guarantee the robot density is to add more robots to the system, which would directly guarantee the method's validity across macroscopic and microscopic instantiations. However, this is naturally not possible. Therefore, changing the collaboration area is a strategy to tackle such a problem, which can only be approximated. Our method uses a scaling factor, Ω, based on the range of sensing and the environment size. There is a special case for k_{ii}, where $X_j = \frac{X_i - 1}{2}$, to account for the fact that robots performing the same task are interacting. For all macroscopic models the collaboration parameters are $k_{12} = k_{31} = 0.002$, $k_{23} = 0.0003$, and $k_{11} = k_{22} = k_{33} = 0.0002$ with estimated relative speeds of $v_{12} = v_{23} = v_{11} = v_{22} = 0.9$ and $v_{31} = v_{33} = 0.5$.

In Control 2, the additional transition rates are not based on spatial interactions, instead p_{ij} is related to how much time a robot is performing a task. Previous work has interpreted such models as a stochastic jump process from one state to another, which can be interpreted as a switch based on sampling a Poisson Distribution with mean related to the transition rate, for more information on this see [17]. For an individual robot, a transition rate, p_{ij}, relates to the next time to switch tasks by taking a random sample from an exponential distribution with a rate of f_{ij} or b_{ji}. The rates are defined in terms of p_{ij} as, $f_{ij} = \frac{1}{N} p_{ij} X_i$ and $b_{ji} = \frac{1}{N} p_{ji} X_j$. For all results of Control 2 we selected transition rates to be the dominant process: $p_{12} = p_{13} = p_{32} = p_{23} = p_{31} = 0.1$.

To evaluate our microscopic instantiation of the macroscopic models, we will benchmark against microscopic coverage control [14]. Coverage control can be formulated by solving the Voronoi partition for each robot in the environment, and then having the robot survey its assigned region. Within each region we consider two planning approaches, the first uses lawnmower patterns similar to [7], and the second is the multi-robot extension of Tan *et al.* [31] which uses the Upper Confidence Bound (UCB) along with predictions from a GP to determine the next location the robot should go. This approach explicitly balances the trade-off between exploration and exploitation.

To evaluate the two coverage control approaches and our two macroscopic controllers we compute the mean squared error between the estimated GP, x_i, and the underlying environmental model used, $\hat{x}_i$, at the end of fixed trials, $mse = \frac{1}{N} \sum_i^N (\hat{x}_i - x_i)^2$. We use two environments for evaluation. The first environment is a 10×10 unit environment with depth map defined as a sum of Gaussian model: means $(2, 1)$, $(5, 8)$, $(7, 3)$, and $(6, 9)$, variances $(1, 2)$, $(2, 1)$, $(0.5, 0.5)$, $(5, 5)$, and amplitudes of 5 for each mean, sigma pair. The second environment uses the underlying GP solved for the experimentally collected river data, and each robot samples from the solved distribution, we limit this environment to a $100x100$m square of the original data. For the sum of Gaussian environment, $\Omega = 0.275$ for $N = 100$, and $\Omega = 0.365$ for $N = 10$. For the river environment $\Omega = 0.415$ for $N = 30$. These values were tuned for our test cases.

V. Results

Figure 4 shows the results for the sum of Gaussian environmental model. In Figures 4a and 4b there are highlighted Voronoi regions, which show that the robots in these cells are

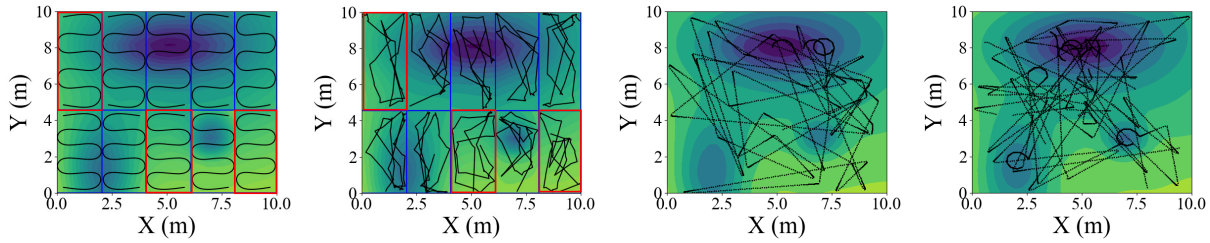

(a) MR Lawnmower Pattern (b) MR UCB (c) Macroscopic C1 (d) Macroscopic C2

Fig. 4: The final GP of all data collected at $t = 100$s and the trajectories, black lines, of each robot where depth data is the sum of Gaussian environmental model. The initial condition is $X(0) = \begin{bmatrix}10 & 0 & 0\end{bmatrix}^T$. The coverage control methods Figures 4a and 4b highlight allocations in red where robots are performing environmental monitoring but are restricted to uninteresting parts of the environment. The macroscopic Figures 4c and 4d highlight 5 randomly selected agent trajectories when executing the explore and exploit tasks where all of these paths at some point interact with deep regions in the environment.

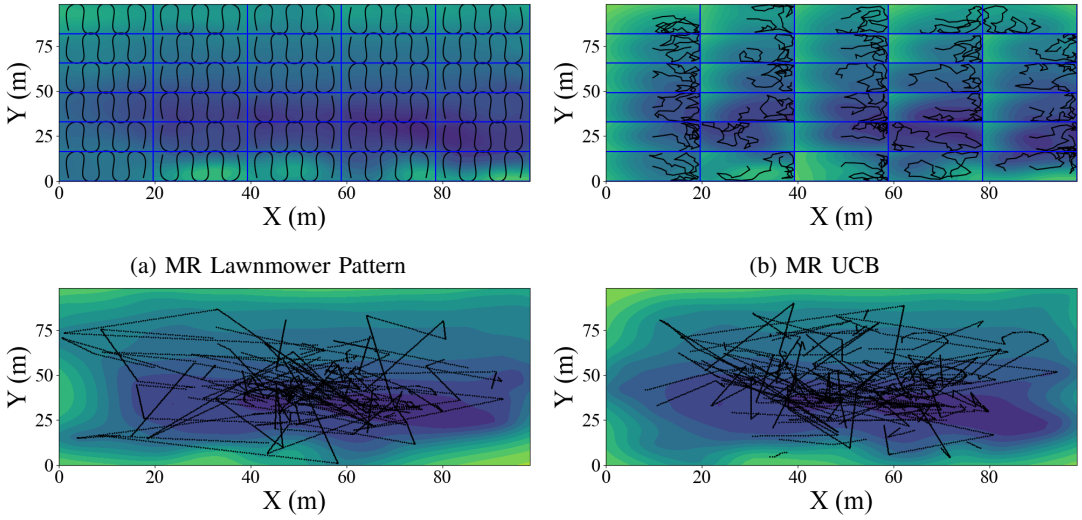

(a) MR Lawnmower Pattern (b) MR UCB

(c) Macroscopic C1 (d) Macroscopic C2

Fig. 5: The final GP of all data collected at $t = 300$s and the trajectory of each robot where depth data is the experimental river data. The initial populations are $X(0) = \begin{bmatrix}30 & 0 & 0\end{bmatrix}^T$. While Figure 5a shows good results, Figure 5b needs more time to have a complete picture of the larger environment. The macroscopic control methods in Figures 5c and 5d show 10 randomly selected agent trajectories, black lines, where the concentration of data is collected in deep parts of the environment.

not necessarily sampling in the most interesting region of the environment. As compared to both macroscopic approaches, Figures 4c and 4d, where five sample robot trajectories are not rigidly assigned to regions and can more freely execute different tasks throughout the environment. The resulting mean squared error of the predicted environmental models across all four methods is in the following table:

	Lawnmower	MR UCB	Macro C1	Macro C2
Env 1	0.028	0.0324	0.013	0.017
Env 2	0.039	1.77	0.93	0.69

In the river environmental data scenario, Figure 5, for the macroscopic solutions we see ten sample trajectories that highlight the flexibility robots have to switch task based on collaboration. Figure 5d shows shorter path segments reflecting a switch to the home task, which is more likely due to time based switching in C2. We believe the high mean squared error for MR-UCB would decrease significantly if more time for each robot was given to explore. Across all environments the collaborative based task switching method performs comparably to coverage control methods, and suggests that instead of naive partitioning of unknown environments a more flexible method which controls the distributions of robots performing tasks is worth considering.

Figure 6 shows three microscopic trials represented as points along with the macroscopic model as solid lines for the uncontrolled method and both control methods. The initial conditions are $X(0) = [100, 0, 0]^T$ for both controlled methods, $X(0) = [40, 30, 30]^T$ for the uncontrolled method, and depth data used the sum of Gaussian environmental model. Figure 6c, has the behavior extinction predicted by Claim 1 when no control is present. Qualitatively, both control methods, Figure 6a and 6b, are close to the predicted population sizes up to $t = 50$ s. At $t > 50$ s, we see a

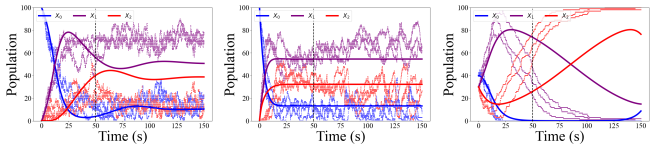

(a) Control 1 (b) Control 2 (c) No Control

Fig. 6: Three microscopic trials represented as dots along corresponding macroscopic continuous model in solid line, and robots sampling from a sum of Gaussian environmental model. At $t = 50\,\text{s}$, the robots switch to a greedy exploitation strategy highlighted by a vertical dashed line.

deviation from our predicted model, we believe this comes from the switch to a greedy exploitation behavior pattern and the breakdown of the *well-mixed* assumption. This is more prominent for C1 where only collaborations are used as shown in Figure 6a.

VI. Conclusion

In this paper, we defined a method for global specification of desired robot distributions for an environmental monitoring scenario. Our results suggest that in unknown environments instead of using individual robot methods where robots might over sample data in uninteresting regions, more flexible collaborative macroscopic ensemble models can be used with similar returns. While our approach was able to perform comparably to existing methods, there are some outstanding challenges, including our understanding of collaboration in non *well-mixed* scenarios. Consider in Figure 6 after $t = 50\,\text{s}$ we see that our model predictions begin to deteriorate. We believe this break down emerges because robots begin to cluster in regions of the environment in a way that hinders the possibility for robot collaboration. Future work aims to address the break-down of the *well-mixed* assumption, since it is relevant across a wide range of tasks.

References

[1] M. Doyle, *The source: How rivers made America and America remade its rivers*. WW Norton & Company, 2018.

[2] M. G. Macklin and J. Lewin, "The rivers of civilization," *Quaternary Science Reviews*, vol. 114, pp. 228–244, 2015.

[3] J. Best, "Anthropogenic stresses on the world's big rivers," *Nature Geoscience*, vol. 12, no. 1, pp. 7–21, 2019.

[4] J. Opperman, G. Grill, and J. Hartmann, "The power of rivers: Finding balance between energy and conservation in hydropower development." 2017.

[5] L. Slater, A. Khouakhi, and R. Wilby, "River channel conveyance capacity adjusts to modes of climate variability," *Scientific reports*, vol. 9, no. 1, pp. 1–10, 2019.

[6] M. Garcia, "Sedimentation engineering: processes, measurements, modeling, and practice." American Society of Civil Engineers, 2008.

[7] N. Karapetyan, J. Moulton, J. S. Lewis, A. Quattrini Li, J. M. O'Kane, and I. Rekleitis, "Multi-robot dubins coverage with autonomous surface vehicles," in *2018 IEEE International Conference on Robotics and Automation (ICRA)*, 2018, pp. 2373–2379.

[8] T. Salam and M. A. Hsieh, "Adaptive sampling and reduced-order modeling of dynamic processes by robot teams," *IEEE Robotics and Automation Letters*, vol. 4, no. 2, pp. 477–484, 2019.

[9] S. Manjanna, A. Q. Li, R. N. Smith, I. Rekleitis, and G. Dudek, "Heterogeneous multi-robot system for exploration and strategic water sampling," in *2018 IEEE International Conference on Robotics and Automation (ICRA)*, 2018, pp. 4873–4880.

[10] M. Duarte, J. Gomes, V. Costa, T. Rodrigues, F. Silva, V. Lobo, M. M. Marques, S. M. Oliveira, and A. L. Christensen, "Application of swarm robotics systems to marine environmental monitoring," in *OCEANS 2016-Shanghai*. IEEE, 2016, pp. 1–8.

[11] S. Manjanna, M. A. Hsieh, and G. Dudek, "Scalable multirobot planning for informed spatial sampling," *Autonomous Robots*, pp. 1–13, 2022.

[12] R. J. Alitappeh and K. Jeddisaravi, "Multi-robot exploration in task allocation problem," *Applied Intelligence*, vol. 52, no. 2, pp. 2189–2211, 2022.

[13] A. Khamis, A. Hussein, and A. Elmogy, "Multi-robot task allocation: A review of the state-of-the-art," *Cooperative Robots and Sensor Networks 2015*, pp. 31–51, 2015.

[14] R. Almadhoun, T. Taha, L. Seneviratne, and Y. Zweiri, "A survey on multi-robot coverage path planning for model reconstruction and mapping," *SN Applied Sciences*, vol. 1, pp. 1–24, 2019.

[15] C. Nam and D. A. Shell, "Analyzing the sensitivity of the optimal assignment in probabilistic multi-robot task allocation," *IEEE Robotics and Automation Letters*, vol. 2, no. 1, pp. 193–200, 2017.

[16] S. Biswal, K. Elamvazhuthi, and S. Berman, "Decentralized control of multi-agent systems using local density feedback," *IEEE Transactions on Automatic Control*, 2021.

[17] T. C. Silva, V. Edwards, and M. A. Hsieh, "Proportional control for stochastic regulation on allocation of multi-robots," *16th International Symposium on Distributed Autonomous Robotic Systems (DARS)*, 2022.

[18] S. Berman, A. Halász, M. A. Hsieh, and V. Kumar, "Optimized stochastic policies for task allocation in swarms of robots," *IEEE transactions on robotics*, vol. 25, no. 4, pp. 927–937, 2009.

[19] T. W. Mather and M. A. Hsieh, "Distributed robot ensemble control for deployment to multiple sites," *Robotics: Science and Systems VII*, 2011.

[20] A. Prorok, M. A. Hsieh, and V. Kumar, "The impact of diversity on optimal control policies for heterogeneous robot swarms," *IEEE Transactions on Robotics*, vol. 33, no. 2, pp. 346–358, 2017.

[21] M. Jeong, J. Harwell, and M. Gini, "Analysis of exploration in swarm robotic systems," in *Intelligent Autonomous Systems 16: Proceedings of the 16th International Conference IAS-16*. Springer, 2022, pp. 445–457.

[22] M. A. Hsieh, A. Halasz, E. D. Cubuk, S. Schoenholz, and A. Martinoli, "Specialization as an optimal strategy under varying external conditions," in *2009 IEEE International Conference on Robotics and Automation*, 2009, pp. 1941–1946.

[23] V. Edwards, T. C. Silva, and M. A. Hsieh, "Stochastic nonlinear ensemble modeling and control for robot team environmental monitoring," *16th International Symposium on Distributed Autonomous Robotic Systems (DARS)*, 2022.

[24] A. K. Li, Y. Mao, S. Manjanna, S. Liu, J. Dhanoa, B. Mehta, V. Edwards, F. C. Ojeda, M. A. Hsieh, M. L. Men, E. Sigg, D. J. Jerolmack, and H. N. Ulloa, "Towards understanding underwater weather events in rivers using autonomous surface vehicles," in *OCEANS 2022, Hampton Roads*, 2022, pp. 1–8.

[25] D. T. Gillespie, "A general method for numerically simulating the stochastic time evolution of coupled chemical reactions," *Journal of computational physics*, vol. 22, no. 4, pp. 403–434, 1976.

[26] D. Pais, C. H. Caicedo-Nunez, and N. E. Leonard, "Hopf bifurcations and limit cycles in evolutionary network dynamics," *SIAM Journal on Applied Dynamical Systems*, vol. 11, no. 4, pp. 1754–1784, 2012.

[27] J. Hofbauer, P. Schuster, K. Sigmund, and R. Wolff, "Dynamical systems under constant organization ii: Homogeneous growth functions of degree p=2," *SIAM Journal on Applied Mathematics*, vol. 38, no. 2, pp. 282–304, 1980.

[28] S. H. Strogatz, *Nonlinear dynamics and chaos: with applications to physics, biology, chemistry, and engineering*. CRC press, 2018.

[29] M. S. Media, "Tides for (schuylkill river) market street bridge." [Online]. Available: https://tides.net/pennsylvania/1591/?year=2022\&month=08

[30] F. Pedregosa, G. Varoquaux, A. Gramfort, V. Michel, B. Thirion, O. Grisel, M. Blondel, P. Prettenhofer, R. Weiss, V. Dubourg, J. Vanderplas, A. Passos, D. Cournapeau, M. Brucher, M. Perrot, and E. Duchesnay, "Scikit-learn: Machine learning in Python," *Journal of Machine Learning Research*, vol. 12, pp. 2825–2830, 2011.

[31] Y. T. Tan, A. Kunapareddy, and M. Kobilarov, "Gaussian process adaptive sampling using the cross-entropy method for environmental sensing and monitoring," in *2018 IEEE International Conference on Robotics and Automation (ICRA)*. IEEE, 2018, pp. 6220–6227.